

Gravitational wave signals from leptoquark-induced first order electroweak phase transitions

Bowen Fu^{1,*} and Stephen F. King^{1,†}

¹*Department of Physics and Astronomy, University of Southampton, SO17 1BJ Southampton, United Kingdom*

(Dated: October 6, 2022)

We consider the extension of the Standard Model (SM) with scalar leptoquarks in $SU(2)$ singlet, doublet and triplet representations. Through the coupling between leptoquark and the SM Higgs field, the electroweak phase transition (EWPT) can turn into first order and consequently produce gravitational wave signals. We compute the required value of the leptoquark-Higgs for first order EWPT to happen and discuss about the possible constraint from Higgs phenomenology. Choosing some benchmarks, we present the strength of the gravitational waves produced during the leptoquark-induced first order EWPT and compare them to detector sensitivities. We find that the $SU(2)$ representations of the leptoquark can be distinguished by gravitational waves in the parameter space where first order EWPT can happen as a function of the Higgs portal coupling.

CONTENTS

I. Introduction	1
II. First order EWPT induced by scalar leptoquarks	2
A. Constraints on the Higgs portal coupling	5
III. Gravitational wave signals	5
IV. Conclusion	8
Acknowledgments	9
A. Production of gravitational waves during a first order phase transition	9
References	10

I. INTRODUCTION

Leptoquarks (LQs) are hypothetical particles that can convert quarks into leptons and vice versa with great interest in elementary particle physics. From the theoretical aspect, it has been predicted naturally by the Pati-Salam unification of quarks and leptons [1, 2] where leptoquark is first raised as well as many other grand unified theories [3–9]. From the experimental side, the existence of leptoquarks is strongly indicated by lepton flavour universality violation (LFUV) in semi-leptonic B decay [10–15]. Besides LFUV, leptoquarks can also be related to a wide variety of phenomena beyond the standard model, including the muon $g - 2$ [16–21], the neutrino mass [22–26] and the W boson mass [27–32].

Despite the theoretical and experimental attraction from leptoquarks, they have not been found by any collider experiment so far. One of the possibilities to find leptoquark is through its connection with Higgs phenomenology [33, 34]. Generically, the scalar leptoquarks can couple to Higgs boson in the scalar potential. After electroweak symmetry breaking, the leptoquark-Higgs operator induces the couplings to the physical Higgs boson which can further affect loop-induced Higgs production and decay processes. Such effects can be probed with the Higgs signal strength measurements at colliders and thus are potential smoking guns for leptoquarks.

At the meantime, the Higgs portal allows leptoquarks to modify the EWPT in the early universe. It has been shown that first order EWPT can be induced by an additional singlet scalar field without any vacuum expectation value (VEV) [35]. And the stochastic gravitational wave background produced during the cosmological phase transition

* B.Fu@soton.ac.uk

† king@soton.ac.uk

can be potentially tested by detectors [36, 37]. This provide us with a new possibility of testing scalar leptoquarks, using a similar approach to the singlet, from cosmic signals.

In this paper, we extend the study of first order EWPT induced by an extra singlet scalar to the case of scalar leptoquarks in $SU(2)$ singlet, doublet and triplet representations, and show how such leptoquarks can affect the EWPT through their coupling to the standard model Higgs boson. By computing the effective scalar potential, we find the range of Higgs portal where eligible first order EWPT can happen for different types of scalar leptoquark with a mass around TeV scale. Then we calculate the gravitational wave background produced during the first order EWPT induced by leptoquark for some benchmark cases and compare it with the detector sensitivities. We found that in some range of the parameter space, the first order EWPT induced by a leptoquark is able to produce gravitational wave signals which are strong enough to be detected.

The paper is organised as follows. In Sec.II, we discuss the first order EWPT induced by leptoquark through the Higgs portal. We also show the constraint from Higgs physics to the parameter space. In Sec.III, we show the gravitation wave signal produced during leptoquark-induced first order EWPT for benchmark points. Finally, we summarise and conclude in Sec.IV.

II. FIRST ORDER EWPT INDUCED BY SCALAR LEPTOQUARKS

In this section, we discuss how first order EWPT can be induced by leptoquarks. The scalar potential of the SM scalar doublet H and an extra complex scalar leptoquark S with a $SU(2)$ index a , corresponding to a singlet, doublet or triplet representation, can be written as

$$V_0 = -\mu^2|H|^2 + \lambda_H|H|^4 + \mu_S^2|S_a|^2 + \lambda_S|S_a|^4 + 2\lambda_{HS}|H|^2|S_a|^2 \quad (1)$$

For simplicity, we only consider the minimal quartic interaction between Higgs and scalar leptoquark in the form of $|H|^2|S|^2$. Other forms of quartic interactions such as $|H^\dagger S|^2$ for $SU(2)$ doublet leptoquark and $H^\dagger(\sigma^i S_i)(\sigma^j S_j)^\dagger H$ for $SU(2)$ triplet leptoquark can lead to mass shifts between the $SU(2)$ components of leptoquarks after spontaneous symmetry breaking (SSB) as well as extra contributions to the thermal mass of the SM Higgs field. Focussing on the field h in $H = (G^+, (h + iG^0)/\sqrt{2})$ which becomes the SM Higgs boson after spontaneous symmetry breaking, the scalar potential becomes

$$V_0 = -\frac{\mu^2}{2}h^2 + \frac{\lambda_H}{4}h^4 + \frac{\mu_S^2}{2}(s_{a,1}^2 + s_{a,2}^2) + \frac{\lambda_S}{4}(s_{a,1}^2 + s_{a,2}^2)^2 + \frac{\lambda_{HS}}{2}h^2(s_{a,1}^2 + s_{a,2}^2) \quad (2)$$

where $S_a = (s_{a,1} + i s_{a,2})/\sqrt{2}$. As the leptoquark is typically heavier than the electroweak scale, we assume $\mu_S^2 > 0$ in this research. Then the leptoquark mass after SSB is $m_S^2 = \mu_S^2 + \lambda_{HS}v_0^2$ with v_0 the standard model Higgs VEV. At tree level, the phase transition is second order as the participation of S does not vary the minimum of the scalar potential. However, by considering the finite temperature effective potential, the existence of a leptoquark modifies the minimum through the Higgs portal at loop order. In this study, we consider the scalar effective potential at one-loop level for simplicity, neglecting higher order effects [38] which may vary the transition strength by 20%. We also neglect renormalisation group corrections which have a smaller effect [39].

At one-loop level, the effective scalar potential receives contribution from zero-temperature correction $\Delta V_0^{1-\text{loop}}$ (Coleman-Weinberg potential) and finite-temperature correction $\Delta V_T^{1-\text{loop}}$ [40]

$$V_{\text{eff}}(h, T) = V_0 + \Delta V_0^{1-\text{loop}}(h) + \Delta V_T^{1-\text{loop}}(h, T). \quad (3)$$

The one-loop zero-temperature correction reads

$$\Delta V_0^{1-\text{loop}}(h) = \sum_{i \in b, f} \frac{n_i}{64\pi^2} \left[m_i^4(h) \left(\ln \frac{m_i^2(h)}{m_i^2(v_0)} - \frac{3}{2} \right) + 2m_i^2(h)m_i^2(v_0) \right], \quad (4)$$

where $m_i^2 = m_{0i}^2 + a_i h^2$ are the shifted masses with

$$m_{0\{t, W, Z, h, G, S\}}^2 = \{0, 0, 0, -\mu^2, -\mu^2, \mu_S^2\}, \quad (5)$$

$$a_{\{t, W, Z, h, G, S\}} = \left\{ \frac{y_t^2}{2}, \frac{g^2}{4}, \frac{g^2 + g'^2}{4}, 3\lambda_H, \lambda_H, \lambda_{HS} \right\}, \quad (6)$$

$$n_{\{t, W, Z, h, G, S\}} = \{-12, 6, 3, 1, 3, n_S\}. \quad (7)$$

The quantity v_0 is the SM Higgs VEV at zero temperature. The degree of freedom n_S in the complex $SU(3)$ triplet S , depending on the $SU(2)$ nature of the leptoquark, can be 6 for $SU(2)$ singlet, 12 for $SU(2)$ doublet or 18 for $SU(2)$ triplet.

The one-loop finite-temperature correction in Eq.3 is

$$\Delta V_T^{1\text{-loop}}(h, T) = \sum_{i \in b} \frac{n_i T^4}{2\pi^2} J_b \left(\frac{m_i^2}{T^2} \right) + \sum_{i \in f} \frac{n_i T^4}{2\pi^2} J_f \left(\frac{m_i^2}{T^2} \right) \quad (8)$$

where b and f stand for bosons and fermions and

$$J_{b/f} \left(\frac{m_i^2}{T^2} \right) = \int_0^\infty dx x^2 \ln \left[1 \mp e^{-\sqrt{x^2 + m_i^2(h)/T^2}} \right], \quad (9)$$

At high temperature $T \gtrsim m_i$, the functions J_b and J_f can be expressed approximately as

$$J_b \left(\frac{m_i^2}{T^2} \right) \simeq -\frac{\pi^4}{45} + \frac{\pi^2 m_i^2}{12 T^2} - \frac{\pi m_i^3}{6 T^3} - \frac{1}{32} \frac{m_i^4}{T^4} \left(\ln \frac{m_i^2}{T^2} - c_b \right) + \dots \quad (10)$$

$$J_f \left(\frac{m_i^2}{T^2} \right) \simeq \frac{7\pi^4}{360} - \frac{\pi^2 m_i^2}{24 T^2} - \frac{1}{32} \frac{m_i^4}{T^4} \left(\ln \frac{m_i^2}{T^2} - c_f \right) + \dots \quad (11)$$

with $c_b \simeq 5.4$ and $c_f \simeq 2.6$. At low temperature $T < m_i$, J_b is exponentially suppressed as its argument increases.

To maintain the perturbativity of gauge couplings at high temperature [41, 42], the so-called ring (daisy) diagrams should be resummed. There are two different methods widely used for resummation. In the Parwani method [43], the shifted masses of bosons in the effective potential are replaced by the Debye masses $M_i^2(h, T) = m_i^2(h) + \Pi_i(T)$, where the self-energies $\Pi_i(T)$ are given by $\Pi_i(T) = b_i T^2$ with [44]

$$b_h = b_G = \frac{3g^2 + g'^2}{16} + \frac{\lambda_H}{2} + \frac{y_t^2}{4} + \frac{n_S \lambda_{HS}}{12}, \quad b_W = b_Z(T) = \frac{11}{6} g^2, \quad b_\gamma = \frac{11}{6} g'^2, \quad (12)$$

$$b_S = \begin{cases} \frac{\lambda_{HS}}{3} + \frac{(n_S + 2)\lambda_S}{12} + \frac{3}{4} g_3^2 + \frac{1}{4} Y^2 + \frac{g'^2}{16} & SU(2)\text{singlet}, \\ \frac{\lambda_{HS}}{3} + \frac{(n_S + 2)\lambda_S}{12} + \frac{3}{4} g_3^2 + \frac{1}{4} Y^2 + \frac{3g^2 + g'^2}{16} & SU(2)\text{ doublet and triplet}. \end{cases} \quad (13)$$

In the Arnold-Espinosa method [45], the replacement only happens in the mass cubic terms. In this paper, we adapt the Parwani method. While the leptoquark coupling Y is typically smaller than unitarity [46], the $SU(3)$ coupling can have significant contribution to the Debye mass of the leptoquarks. However, the contributions, not only from the $SU(3)$ coupling but also from other gauge couplings, play the same role as the self-interaction coupling λ_S in phase transition and thus can be absorbed effectively by λ_S , turning it into $\tilde{\lambda}_S$. As λ_S is unconstrained, relevant discussion is commonly avoided by fixing it to certain value [35, 47]. Here, we consider the contributions to the thermal mass from the gauge couplings and leptoquark-fermion couplings as an effective contribution to the quartic coupling λ_S and fix the resulting effective $\tilde{\lambda}_S$ to be 2.

When the phase transition happens at a low temperature, the effective potential can develop an imaginary part as the thermal masses of Goldstone bosons become negative. It has been pointed out in [48] that such an imaginary part remarks the decay rate of the quantum state minimising the Hamiltonian.

In the simplest case, the sufficient conditions for a eligible first order EWPT to occur are

1. The electroweak minimum is the true minimum at zero temperature $T = 0$ and $h = 0$ is a local maximum ($V''(0, 0) < 0$).
2. At the temperature T_2 that $h = 0$ transfer from a local maximum to a local minimum, there is another non-zero local minimum.

The first condition ensures that the phase transition is completed today. If $h = 0$ is a local minimum at zero temperature, the phase transition can only happen through tunnelling and the probability is too low for the vacuum to transfer to the electroweak vacuum until today. The second condition ensures that there are two minima existing simultaneously during the phase transition. In a scenario satisfying both of the conditions, the two minima of the scalar potential are degenerate at a critical temperature T_c . The allowed parameter spaces for first-order phase transition to happen are shown as the coloured regions in Fig.1. The strength of the transition can be estimated by the ratio of the non-zero VEV and the critical temperature, v_c/T_c , which is shown as the colour in Fig.1. Above the coloured regions, the first order EWPT is not eligible as condition 1 is not satisfied; below the coloured regions, first order EWPT cannot happen because condition 2 is not satisfied.

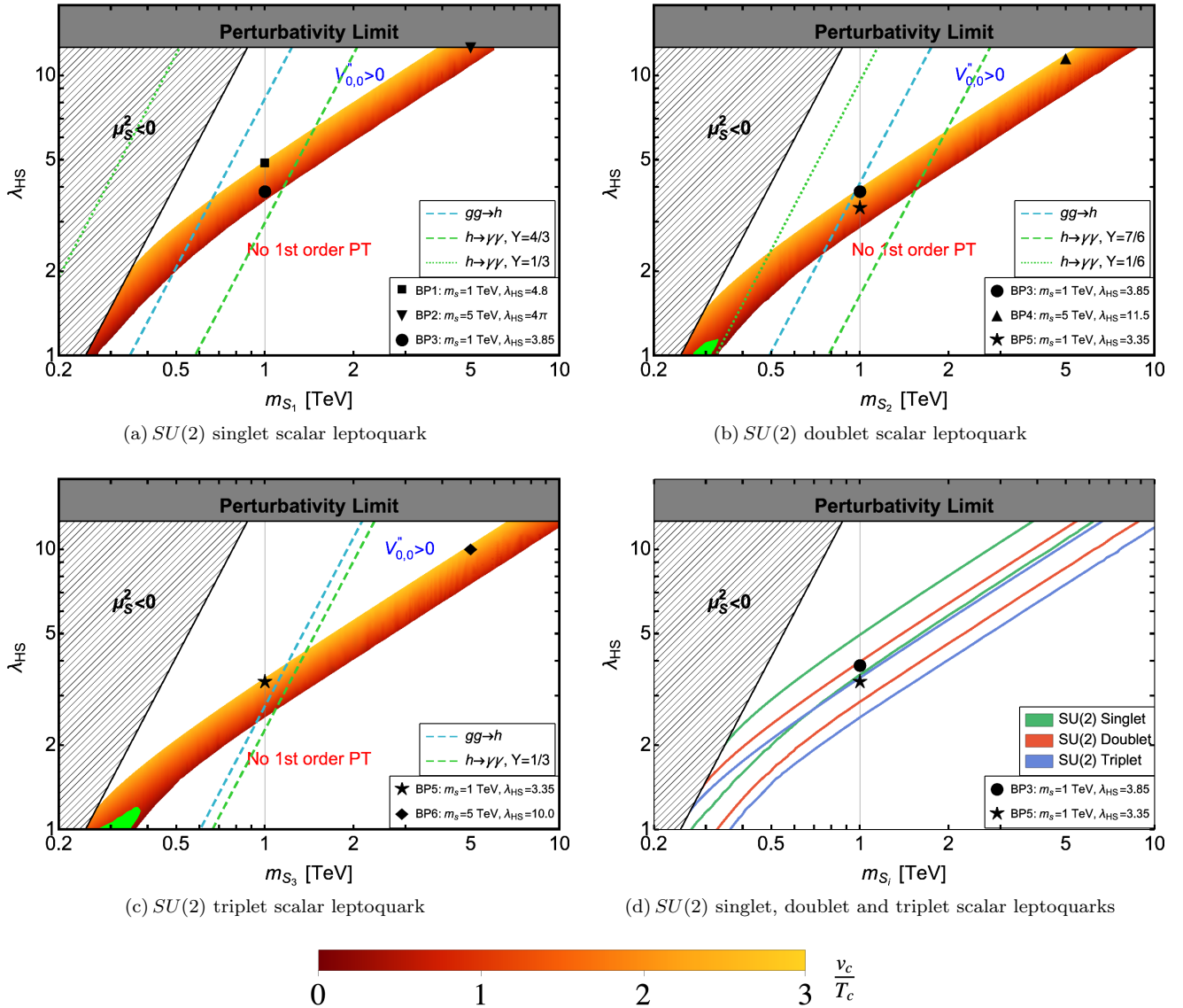


FIG. 1. Allowed parameter space for first-order phase transition induced by different types of scalar leptoquark.

In Fig.1(a) to Fig.1(c), the required coupling for first order EWPT increases as the leptoquark becomes heavier in each $SU(2)$ representation of leptoquark. By comparing different panels and also by comparing the lines with different colours in Fig.1(d), it can be figured out that the Higgs portal coupling required for first order EWPT becomes smaller as the dimension of the leptoquark $SU(2)$ representation increases. Empirical expressions of the interesting parameter spaces can be obtained when the leptoquark is heavy. For leptoquark mass above 1 TeV, the allowed Higgs portal for eligible first order EWPT to happen is roughly between $\{2.87, 4.00\} \times (m_{S_2}/1 \text{ TeV})^{0.679}$ for doublet leptoquark and between $\{2.52, 3.50\} \times (m_{S_3}/1 \text{ TeV})^{0.676}$ for triplet leptoquark.

A more complicated case can occur when the scalar potential develops two non-zero minima simultaneously after the temperature drops below T_2 . In such a case, the scalar configuration transfer to the nearest non-zero minimum continuously through second order phase transition and tunnel to the larger non-zero minimum through second order phase transition. The regions where such cases happen are marked as green in Fig.1(b) and Fig.1(c). However, as the leptoquark is typically above 1 TeV, such regions are not of interest in this study.

A. Constraints on the Higgs portal coupling

The new interaction between a scalar leptoquark and the Higgs doublet can affect the Higgs boson production and decay processes. The discrepancy between SM prediction and experimental measurement is commonly characterised by the \varkappa -factor, defined as $\varkappa_i = \sqrt{\Gamma_i^{\text{exp}}/\Gamma_i^{\text{SM}}}$ [49, 50]. The loop-induced contribution from leptoquark to the Higgs boson decay process into photons and the gluon-gluon production of Higgs boson are given by [34]

$$\varkappa_g = 1 + 0.24 \frac{\lambda_{HS} v^2}{m_S^2} N_S \quad (14)$$

$$\varkappa_\gamma = 1 - 0.052 \frac{\lambda_{HS} v^2}{m_S^2} N_c \sum_i Q_i^2 \quad (15)$$

where the sum is taken over all $SU(2)$ components of the leptoquark and Q_i is the electric charge of the i th component. N_S is the number of the leptoquark $SU(2)$ components. The experimental measurements by the ATLAS collaboration are $\varkappa_g = 1.01_{-0.09}^{+0.11}$ and $\varkappa_\gamma = 1.02_{-0.07}^{+0.08}$ [51]. Similar contribution appears in the decay channel of Higgs into a Z boson and a photon as well, in the form of [34]

$$\varkappa_{Z\gamma} = 1 + 0.036 \frac{\lambda_{HS} v^2}{m_S^2} N_c \sum_i Q_i (I_i^W - 0.23Q_i) \quad (16)$$

where I_i^W is the value of the weak isospin of the leptoquark. The value of $\varkappa_{Z\gamma}$ measured by CMS collaboration is $1.65_{-0.37}^{+0.34}$ [52]. Despite abundant collider phenomena caused by the Higgs portal to leptoquarks, none of the observables can constrain the portal coupling restrictedly. When multiple leptoquarks appear in a model, the contributions from different types of leptoquarks can have opposite contributions to the \varkappa parameters above. In order to visualise the effects of these observables, we consider the collider constraints under the assumption of a single leptoquark multiplet and show the maximal values of the Higgs portal allowed by $h \rightarrow \gamma\gamma$ and $gg \rightarrow h$ as the dashed and dotted lines in Fig.1(a) to Fig.1(c). While the $gg \rightarrow h$ cross section is affected by the $SU(2)$ representation of the leptoquark, the $h \rightarrow \gamma\gamma$ cross section depends on the electric charge. For scalar leptoquark, assuming direct interaction to SM fermions, there are two different possible assignments of hypercharge for $SU(2)$ singlet and doublet and one assignment for $SU(2)$ triplet [53]: 4/3 or 1/3 for singlet, 7/6 or 1/6 for doublet and 1/3 for triplet. Although those constraints are currently weak, they are expected to be improved foreseeably by future experiments like HL-LHC [54], FCC [55, 56], ILC [57] and CEPC [58, 59]. Moreover, the Higgs portal coupling also affects flavour violating processes like the $h \rightarrow \mu\tau$ or $\tau \rightarrow \mu\gamma$ decay which can be tested by precious measurements at colliders [34, 60].

III. GRAVITATIONAL WAVE SIGNALS

During a first-order phase transition, the scalar field configuration transfer from zero vacuum to non-zero vacuum locally in the form of bubbles through tunnelling. The scalar bubbles can then move, collide and expand. Sound waves and magnetohydrodynamic turbulence can be produced after the collision of bubbles. The gravitational wave can be produced through three different mechanisms [36, 37]: **collision** of the scalar bubbles, overlap of the **sound wave** in the plasma and the fluid **turbulence**. The total gravitational wave spectrum is the sum of the three contributions

$$\Omega_{\text{tot}}(f)h^2 = \Omega_{\text{coll}}(f)h^2 + \Omega_{\text{sw}}(f)h^2 + \Omega_{\text{turb}}(f)h^2. \quad (17)$$

All three contributions depend on the phase transition dynamics which is described by four key parameters: the wall velocity v_w , the inverse phase transition duration β/\mathcal{H}_* , the phase transition strength α_{T_*} and the transition temperature T_* . After these parameters are determined, the gravitational wave spectrum can be computed using results from numerical simulations.

The crucial step in computing these key parameters is to compute the Euclidean action. To find the Euclidean action which is defined as the spacial integration of the effective Lagrangian, a solution of the Euclidean equation of motion is required, which is generally not solvable analytically. For further details see Appendix A. A common treatment for particles of electroweak scale or below is to make an approximation using Eq.(10) and Eq.(11) after which the effective potential can be simplified into a quartic function of the scalar field and a semi-analytical bounce solution can be derived [61, 62]. However, as the leptoquark is typically above TeV scale [63–66], the one-loop finite-temperature correction from leptoquark is exponentially suppressed and thus negligible. On the other hand, no eligible expansion can be made to the one-loop zero-temperature correction from leptoquark in the parameter space of interest. Therefore we choose to solve the Euclidean equation of motion numerically in this work.

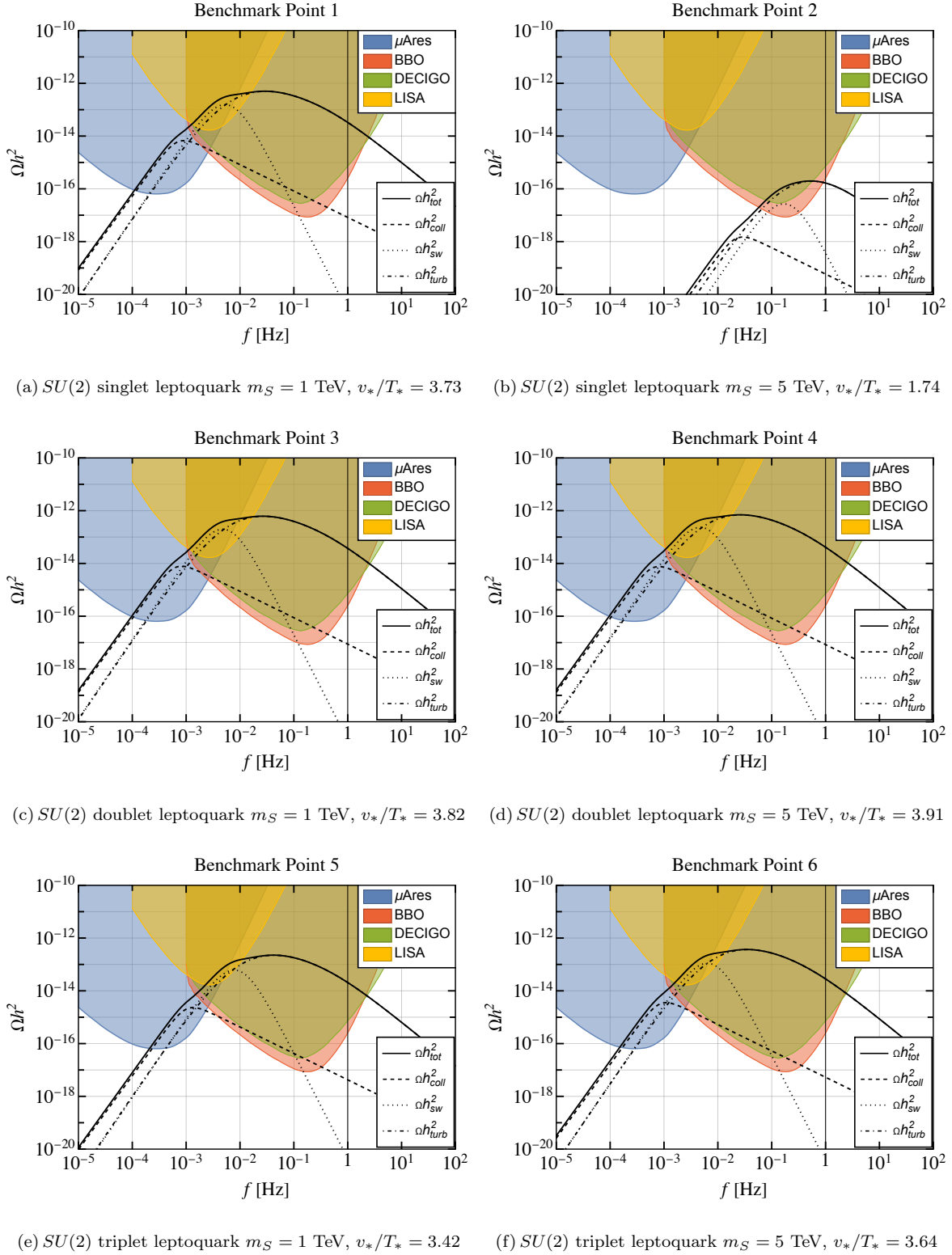


FIG. 2. Gravitational wave signals for difference benchmark cases. The left panels show the strongest gravitational wave signals from first order EWPT induced by 1 TeV leptoquarks for $SU(2)$ singlet, doublet and triplet from top to bottom. The right panels show similar results for 5 TeV leptoquarks.

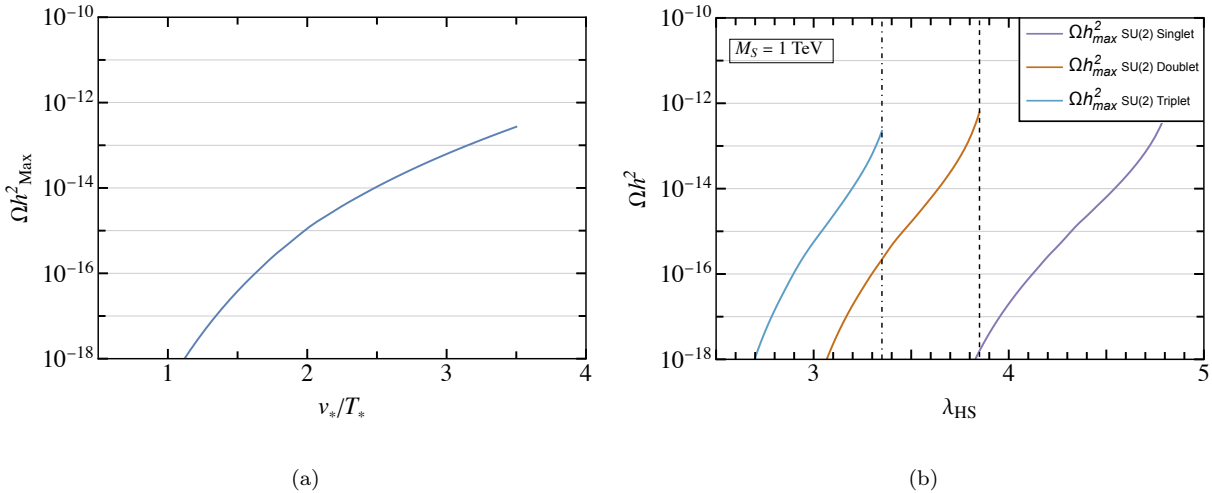


FIG. 3. Left panel: Maximal strength of gravitational wave produced as a function of transition strength v_*/T_* . Right panel: Maximal strength of gravitational wave produced by first order EWPT induced by different type of leptoquarks of 1 TeV as a function of the Higgs portal coupling.

In Fig. 2, we show the gravitational wave produced from first order EWPT for six benchmark cases. From top to bottom, the benchmark cases in each row are chosen for $SU(2)$ singlet, doublet and triplet leptoquark. For each $SU(2)$ representation, the strongest gravitational wave signals that leptoquark-induced first order EWPT can produce when the leptoquark mass is 1 TeV and 5 TeV are presented on the left and right panels respectively. In all the cases, the gravitational wave signals can be detected by BBO [67], DECIGO [68, 69], while LISA [36] and μAres [70] can potentially find the signal in Benchmark Point 1 for singlet leptoquark. We also show the gravitational waves produced by different sources during the phase transition independently. In most of the frequency range, the gravitational wave is dominantly produced by the magnetohydrodynamic (MHD) turbulence.

By comparing panels, it can be observed that only the shape of the gravitational wave spectrum for 5 TeV $SU(2)$ singlet leptoquarks shows a significant difference from the others. In fact, the result follows from the fact that the gravitational wave produced from first order EWPT relies on the strength of the transition. To illustrate the relation more explicitly, we show the dependence of gravitational wave signal peak values on the strength of the phase transition in Fig. 3. Here, instead of v_c/T_c in the previous section, the phase transition strength is evaluated by the ratio of the non-zero minimum of the scalar potential and temperature when the phase transition happens, i.e. when the probability of bubble nucleation is significant. The temperature T_* is defined by the temperature when one bubble is nucleated per unit volume per unit time and the non-zero VEV at T_* is denoted as v_* . We find that the gravitational wave is testable when the phase transition strength is roughly larger than 1.34, corresponding to the Higgs portal roughly larger than $3.95 \times (m_{S_1}/1 \text{ TeV})^{0.685}$ in the singlet case, $3.17 \times (m_{S_2}/1 \text{ TeV})^{0.679}$ in the doublet case and $2.79 \times (m_{S_3}/1 \text{ TeV})^{0.676}$ in the triplet case. In the case with a 5 TeV $SU(2)$ singlet leptoquark, the Higgs portal is constrained by its perturbativity limit and as a consequence, the strongest gravitational wave signal that eligible first order EWPT can produce is less than the other cases.

For the same benchmark point, the gravitational wave produced during first order EWPT induced by leptoquark with a smaller dimension is stronger. In Fig. 4, we choose the benchmark points 3 and 5 in Fig. 1 and show the gravitational wave produced during singlet- and doublet-induced first order EWPT for the former case and the gravitational wave produced during doublet- and triplet-induced first order EWPT for the later one. It is clear that for the same coupling, the first order EWPT induced by the $SU(2)$ multiplet with a higher dimension produces stronger gravitational waves. Supposing the Higgs portal is measured to be in the region where first-order phase transition appears by future collider experiments, the gravitational waves detection provides an alternative method to further test the Higgs portal as well as determine the $SU(2)$ representation of leptoquarks.

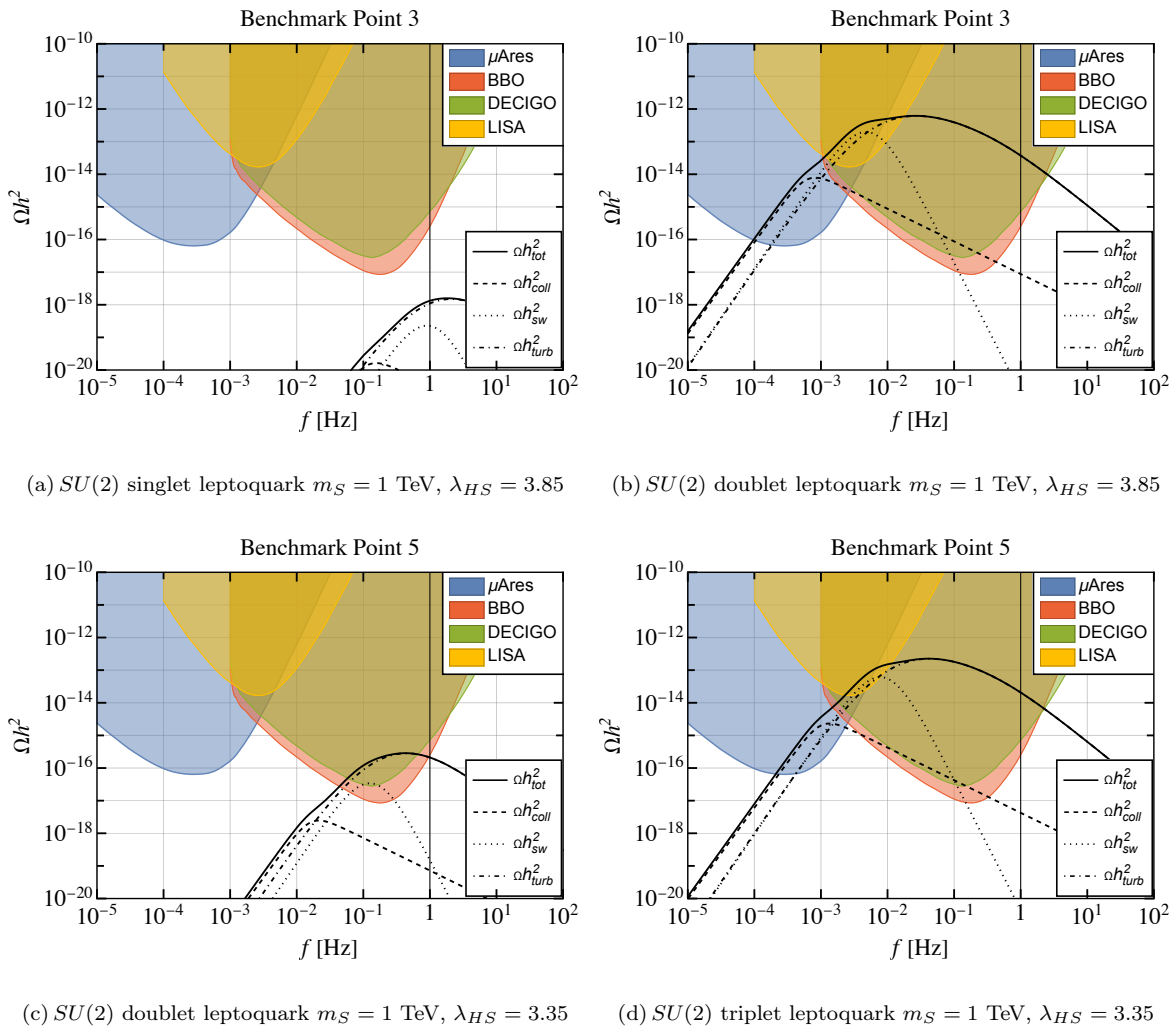


FIG. 4. Gravitational wave signals for the same benchmark cases in different $SU(2)$ representations. The upper panels show the gravitational wave signals for a benchmark case when the leptoquark is $SU(2)$ singlet and doublet. The lower panels show the gravitational wave signals for another benchmark case when the leptoquark is $SU(2)$ doublet and triplet.

IV. CONCLUSION

In this paper, we have explored the possibility that first order EWPT induced by the coupling between a scalar leptoquark and the SM Higgs boson produces detectable gravitational wave signals. We have considered different $SU(2)$ representations of the scalar leptoquark, including singlet, doublet and triplet. Despite the lack of VEV for leptoquark itself, a first order EWPT can be induced due to the 1-loop order effects. In general, with first order EWPTs, gravitational waves can be produced by multiple processes in the dynamical evolution of the scalar bubbles. The resulting gravitational waves form a stochastic background that can be probed by gravitational wave detectors.

We have calculated the effective potential of the SM Higgs field in the presence of a scalar leptoquark, including tree level and 1-loop level contributions as well as the resummation over the ring/daisy diagrams. By applying the conditions for first order EWPT, we have found that the leptoquark can induce a first order EWPT in the parameter space allowed by collider constraints and can be tested by future Higgs precision experiments. Enhanced by the internal degree of freedom of the particular leptoquark, we found that the leptoquark in the $SU(2)$ representation with a higher dimension requires smaller coupling in order to trigger a first order EWPT.

We have followed the standard procedure to compute the gravitational wave spectrum during first order EWPTs. It turns out that the gravitational wave spectrum is mainly determined by the strength of the phase transition characterised by the ratio of the non-zero VEV and the temperature at the time that the transition happens. However,

due to the difference in internal degrees of freedom, the strengths of first order EWPTs induced by leptoquarks with the same masses and Higgs portal couplings but different $SU(2)$ nature are different. Since the gravitational wave signals differ, this provides a possibility to determine the $SU(2)$ representation of the leptoquarks through the observations of gravitational wave in particular regions of parameter space.

ACKNOWLEDGMENTS

BF acknowledges the Chinese Scholarship Council (CSC) Grant No. 201809210011 under agreements [2018]3101 and [2019]536. SFK acknowledges the STFC Consolidated Grant ST/L000296/1 and the European Union's Horizon 2020 Research and Innovation programme under Marie Skłodowska-Curie grant agreement HIDDEN European ITN project (H2020-MSCA-ITN-2019//860881-HIDDEN).

Appendix A: Production of gravitational waves during a first order phase transition

As a beginning to discuss the phase transition dynamics, we need to determine the transition temperature T_* , which is commonly considered to be approximately equivalent to the nucleation temperature. By definition, the nucleation temperature T_n is the temperature at which the probability of nucleating a bubble per unit volume per unit time is of order 1 [40], which can be roughly expressed as $\Gamma(T) \simeq \mathcal{H}^4(T)$ with \mathcal{H} the Hubble parameter [71, 72]. The bubble nucleation rate Γ is given by

$$\Gamma(T) = A(T)e^{-S_E(T)}, \quad (\text{A1})$$

where S_E is the Euclidean action and A is a dynamical prefactor of order T^4 up an $O(1)$ factor [73]. At finite temperature, the four-dimensional euclidean action S_E can be directly related to the three-dimensional Euclidean action S_3 by the relation $S_E = S_3/T$. With the $O(3)$ symmetry at high temperature, S_3 is defined as

$$S_3 = 4\pi \int_0^\infty s^2 \left[\frac{1}{2} \left(\frac{dh}{ds} \right)^2 + V_{\text{eff}}(h) \right] ds, \quad (\text{A2})$$

Thus the Euclidean equation of motion reads

$$\frac{d^2 h}{ds^2} + \frac{2}{s} \frac{dh}{ds} - \frac{dV_{\text{eff}}}{dh} = 0 \quad (\text{A3})$$

with boundary conditions

$$\left. \frac{dh}{ds} \right|_{s=0} = 0, \quad \text{and} \quad \lim_{s \rightarrow \infty} h(s) = 0. \quad (\text{A4})$$

Given T_* and S_E , the inverse phase transition duration can be expressed as

$$\frac{\beta}{\mathcal{H}_*} = T \left. \frac{dS_E(T)}{dT} \right|_{T=T_*}, \quad (\text{A5})$$

where \mathcal{H}_* is the Hubble parameter at T_* . The phase transition strength α_{T_*} is the ratio of the latent heat to the radiation energy density at the transition temperature, i.e. $\alpha_{T_*} = \mathcal{L}(T_*)/\rho(T_*)$. The latent heat is

$$\mathcal{L}(T) = - \left(V_{\text{eff}}^\emptyset(T) - V_{\text{eff}}(0, T) \right) + T \frac{d}{dT} \left(V_{\text{eff}}^\emptyset(T) - V_{\text{eff}}(0, T) \right) \quad (\text{A6})$$

with $V_{\text{eff}}^\emptyset(T)$ the height of effective potential at the non-zero minimum. Depending on whether the bubble wall reaches a relativistic terminal velocity or not, it can either run away or not [74]. A criterion to determine if the bubble wall can run away is to compare the value of α_{T_*} and $\alpha_\infty \simeq 4.9 \times 10^{-3} (h_*/T_*)^2$ where h_* is the VEV of the Higgs field inside the bubbles [36]. If $\alpha_{T_*} > \alpha_\infty$, it is possible to have a runaway bubble [75]. In the case of a non-runaway bubble, we adopt the expression of the wall velocity in [76]

$$v_w = \frac{\sqrt{1/3} + \sqrt{\alpha_{T_*}^2 + 2\alpha_{T_*}/3}}{1 + \alpha_{T_*}}. \quad (\text{A7})$$

In the case of a runaway bubble, we simply assume the wall velocity equals the speed of light as it is ultra-relativistic.

The contributions to the GW spectrum from different sources are given by [36]

$$\Omega_{\text{coll}}(f)h^2 = 1.67 \times 10^{-5} \left(\frac{0.11v_w^3}{0.42 + v_w^2} \right) \left(\frac{\kappa_\phi \alpha_{T_*}}{1 + \alpha_{T_*}} \right)^2 \left(\frac{\mathcal{H}_*}{\beta} \right)^2 \left(\frac{100}{g_*} \right)^{\frac{1}{3}} S_{\text{coll}}(f), \quad (\text{A8})$$

$$\Omega_{\text{sw}}(f)h^2 = 2.65 \times 10^{-6} \left(\frac{\kappa_v \alpha_{T_*}}{1 + \alpha_{T_*}} \right)^2 \left(\frac{\mathcal{H}_*}{\beta} \right) \left(\frac{100}{g_*} \right)^{\frac{1}{3}} v_w S_{\text{sw}}(f), \quad (\text{A9})$$

$$\Omega_{\text{turb}}(f)h^2 = 3.35 \times 10^{-4} \left(\frac{\kappa_t \alpha_{T_*}}{1 + \alpha_{T_*}} \right)^{\frac{3}{2}} \left(\frac{\mathcal{H}_*}{\beta} \right) \left(\frac{100}{g_*} \right)^{\frac{1}{3}} v_w S_{\text{turb}}(f). \quad (\text{A10})$$

where the κ_ϕ , κ_v and κ_t are the efficiency factors. In the case of non-runaway bubbles, the contribution to gravitational wave spectrum is negligible and the efficiency factors for sound wave and turbulence contributions are

$$\kappa_v = \frac{\alpha_{T_*}}{0.73 + 0.083\sqrt{\alpha_{T_*}} + \alpha_{T_*}} \quad \text{and} \quad \kappa_t = \epsilon \kappa_v. \quad (\text{A11})$$

ϵ is the fraction of bulk motion that is turbulent, which is commonly taken to be 0.05 or 0.1 [36, 77, 78]. In the case of runaway bubbles,

$$\kappa_\phi = 1 - \frac{\alpha_\infty}{\alpha_{T_*}}, \quad \kappa_v = \frac{\alpha_\infty}{\alpha_{T_*}} \frac{\alpha_\infty}{0.73 + 0.083\sqrt{\alpha_\infty} + \alpha_\infty} \quad \text{and} \quad \kappa_t = \epsilon \kappa_v. \quad (\text{A12})$$

The spectral form functions S_{coll} , S_{sw} and S_{turb} read

$$S_{\text{coll}}(f) = 3.8 \left(\frac{f}{f_{\text{coll}}} \right)^{2.8} \left[1 + 2.8 \left(\frac{f}{f_{\text{coll}}} \right)^{3.8} \right]^{-1}, \quad (\text{A13})$$

$$S_{\text{sw}}(f) = \left(\frac{f}{f_{\text{sw}}} \right)^3 \left(\frac{7}{4 + 3f^2/f_{\text{sw}}^2} \right)^{\frac{7}{2}}, \quad (\text{A14})$$

$$S_{\text{turb}}(f) = \left(\frac{f}{f_{\text{turb}}} \right)^3 \left(1 + \frac{f}{f_{\text{turb}}} \right)^{-\frac{11}{3}} \left(1 + 8\pi \frac{f}{\mathcal{H}_*} \right)^{-1}, \quad (\text{A15})$$

where f_{coll} , f_{sw} and f_{turb} are the peak frequencies in the three scenarios given by

$$f_{\text{coll}} = 16.5 \mu\text{Hz} \frac{0.62}{1.8 + 0.1v_w + v_w^2} \left(\frac{\beta}{\mathcal{H}_*} \right) \left(\frac{T_*}{100 \text{ GeV}} \right) \left(\frac{g_*}{100} \right)^{\frac{1}{6}}, \quad (\text{A16})$$

$$f_{\text{sw}} = 19 \mu\text{Hz} \frac{1}{v_w} \left(\frac{\beta}{\mathcal{H}_*} \right) \left(\frac{T_*}{100 \text{ GeV}} \right) \left(\frac{g_*}{100} \right)^{\frac{1}{6}}, \quad (\text{A17})$$

$$f_{\text{turb}} = 27 \mu\text{Hz} \frac{1}{v_w} \left(\frac{\beta}{\mathcal{H}_*} \right) \left(\frac{T_*}{100 \text{ GeV}} \right) \left(\frac{g_*}{100} \right)^{\frac{1}{6}}. \quad (\text{A18})$$

-
- [1] J.C. Pati and A. Salam, *Unified Lepton-Hadron Symmetry and a Gauge Theory of the Basic Interactions*, *Phys. Rev. D* **8** (1973) 1240.
- [2] J.C. Pati and A. Salam, *Lepton Number as the Fourth Color*, *Phys. Rev. D* **10** (1974) 275.
- [3] G. Senjanovic and A. Sokorac, *Light Leptoquarks in SO(10)*, *Z. Phys. C* **20** (1983) 255.
- [4] W. Buchmuller and D. Wyler, *Constraints on SU(5) Type Leptoquarks*, *Phys. Lett. B* **177** (1986) 377.
- [5] P.H. Frampton, *Light leptoquarks as possible signature of strong electroweak unification*, *Mod. Phys. Lett. A* **7** (1992) 559.
- [6] S.S. Gershtein, A.A. Likhoded and A.I. Onishchenko, *TeV-scale leptoquarks from GUTs/string/M-theory unification*, *Phys. Rept.* **320** (1999) 159.
- [7] J. Fuentes-Martin, G. Isidori, J. Pagès and B.A. Stefanek, *Flavor non-universal Pati-Salam unification and neutrino masses*, *Phys. Lett. B* **820** (2021) 136484 [2012.10492].
- [8] S.F. King, *Twin Pati-Salam theory of flavour with a TeV scale vector leptoquark*, *JHEP* **11** (2021) 161 [2106.03876].
- [9] M. Fernández Navarro and S.F. King, *B-anomalies in a twin Pati-Salam theory of flavour*, 2209.00276.
- [10] LHCb collaboration, *Search for lepton-universality violation in $B^+ \rightarrow K^+ \ell^+ \ell^-$ decays*, *Phys. Rev. Lett.* **122** (2019) 191801 [1903.09252].
- [11] BELLE collaboration, *Measurement of $\mathcal{R}(D)$ and $\mathcal{R}(D^*)$ with a semileptonic tagging method*, *Phys. Rev. Lett.* **124** (2020) 161803 [1910.05864].

- [12] LHCb collaboration, *Test of lepton universality in beauty-quark decays*, *Nature Phys.* **18** (2022) 277 [2103.11769].
- [13] LHCb collaboration, *Tests of lepton universality using $B^0 \rightarrow K_S^0 \ell^+ \ell^-$ and $B^+ \rightarrow K^{*+} \ell^+ \ell^-$ decays*, *Phys. Rev. Lett.* **128** (2022) 191802 [2110.09501].
- [14] A. Angelescu, D. Bećirević, D.A. Faroughy, F. Jaffredo and O. Sumensari, *Single leptoquark solutions to the B-physics anomalies*, *Phys. Rev. D* **104** (2021) 055017 [2103.12504].
- [15] D. Bećirević, I. Doršner, S. Fajfer, D.A. Faroughy, F. Jaffredo, N. Košnik et al., *On a model with two scalar leptoquarks $-R_2$ and S_3* , **2206.09717**.
- [16] K.-m. Cheung, *Muon anomalous magnetic moment and leptoquark solutions*, *Phys. Rev. D* **64** (2001) 033001 [hep-ph/0102238].
- [17] E. Coluccio Leskow, G. D'Ambrosio, A. Crivellin and D. Müller, *$(g-2)_\mu$, lepton flavor violation, and Z decays with leptoquarks: Correlations and future prospects*, *Phys. Rev. D* **95** (2017) 055018 [1612.06858].
- [18] A. Crivellin, D. Müller and F. Saturnino, *Flavor Phenomenology of the Leptoquark Singlet-Triplet Model*, *JHEP* **06** (2020) 020 [1912.04224].
- [19] P. Athron, C. Balázs, D.H.J. Jacob, W. Kotlarski, D. Stöckinger and H. Stöckinger-Kim, *New physics explanations of a_μ in light of the FNAL muon $g-2$ measurement*, *JHEP* **09** (2021) 080 [2104.03691].
- [20] M. Du, J. Liang, Z. Liu and V.Q. Tran, *A vector leptoquark interpretation of the muon $g-2$ and B anomalies*, **2104.05685**.
- [21] S.-L. Chen, W.-w. Jiang and Z.-K. Liu, *Combined explanations of B-physics anomalies, $(g-2)_{e,\mu}$ and neutrino masses by scalar leptoquarks*, **2205.15794**.
- [22] U. Mahanta, *Neutrino masses and mixing angles from leptoquark interactions*, *Phys. Rev. D* **62** (2000) 073009 [hep-ph/9909518].
- [23] F.F. Deppisch, S. Kulkarni, H. Päs and E. Schumacher, *Leptoquark patterns unifying neutrino masses, flavor anomalies, and the diphoton excess*, *Phys. Rev. D* **94** (2016) 013003 [1603.07672].
- [24] O. Popov and G.A. White, *One Leptoquark to unify them? Neutrino masses and unification in the light of $(g-2)_\mu$, $R_{D^{(*)}}$ and R_K anomalies*, *Nucl. Phys. B* **923** (2017) 324 [1611.04566].
- [25] Y. Cai, J. Gargalionis, M.A. Schmidt and R.R. Volkas, *Reconsidering the One Leptoquark solution: flavor anomalies and neutrino mass*, *JHEP* **10** (2017) 047 [1704.05849].
- [26] P.S. Bhupal Dev, R. Mohanta, S. Patra and S. Sahoo, *Unified explanation of flavor anomalies, radiative neutrino masses, and ANITA anomalous events in a vector leptoquark model*, *Phys. Rev. D* **102** (2020) 095012 [2004.09464].
- [27] A. Crivellin, D. Müller and F. Saturnino, *Leptoquarks in oblique corrections and Higgs signal strength: status and prospects*, *JHEP* **11** (2020) 094 [2006.10758].
- [28] A. D'Alise et al., *Standard model anomalies: lepton flavour non-universality, $g-2$ and W-mass*, *JHEP* **08** (2022) 125 [2204.03686].
- [29] P. Athron, A. Fowlie, C.-T. Lu, L. Wu, Y. Wu and B. Zhu, *The W boson Mass and Muon $g-2$: Hadronic Uncertainties or New Physics?*, **2204.03996**.
- [30] K. Cheung, W.-Y. Keung and P.-Y. Tseng, *Isodoublet vector leptoquark solution to the muon $g-2$, R_K, K^* , RD, D^* , and W-mass anomalies*, *Phys. Rev. D* **106** (2022) 015029 [2204.05942].
- [31] A. Bhaskar, A.A. Madathil, T. Mandal and S. Mitra, *Combined explanation of W-mass, muon $g-2$, $R_{K^{(*)}}$ and $R_{D^{(*)}}$ anomalies in a singlet-triplet scalar leptoquark model*, **2204.09031**.
- [32] S.-P. He, *A leptoquark and vector-like quark extended model for the simultaneous explanation of the W boson mass and muon $g-2$ anomalies*, **2205.02088**.
- [33] S. Kolb, M. Hirsch and H.V. Klapdor-Kleingrothaus, *Bounds on leptoquark parameters with nonvanishing leptoquark Higgs couplings*, *Phys. Lett. B* **391** (1997) 131.
- [34] I. Doršner, S. Fajfer, A. Greljo, J.F. Kamenik and N. Košnik, *Physics of leptoquarks in precision experiments and at particle colliders*, *Phys. Rept.* **641** (2016) 1 [1603.04993].
- [35] D. Curtin, P. Meade and C.-T. Yu, *Testing Electroweak Baryogenesis with Future Colliders*, *JHEP* **11** (2014) 127 [1409.0005].
- [36] C. Caprini et al., *Science with the space-based interferometer eLISA. II: Gravitational waves from cosmological phase transitions*, *JCAP* **04** (2016) 001 [1512.06239].
- [37] D.J. Weir, *Gravitational waves from a first order electroweak phase transition: a brief review*, *Phil. Trans. Roy. Soc. Lond. A* **376** (2018) 20170126 [1705.01783].
- [38] L. Niemi, P. Schicho and T.V.I. Tenkanen, *Singlet-assisted electroweak phase transition at two loops*, *Phys. Rev. D* **103** (2021) 115035 [2103.07467].
- [39] P. Schicho, T.V.I. Tenkanen and G. White, *Combining thermal resummation and gauge invariance for electroweak phase transition*, **2203.04284**.
- [40] M. Quiros, *Finite temperature field theory and phase transitions*, in *ICTP Summer School in High-Energy Physics and Cosmology*, pp. 187–259, 1, 1999 [hep-ph/9901312].
- [41] A.D. Linde, *Infrared Problem in Thermodynamics of the Yang-Mills Gas*, *Phys. Lett. B* **96** (1980) 289.
- [42] D. Croon, O. Gould, P. Schicho, T.V.I. Tenkanen and G. White, *Theoretical uncertainties for cosmological first-order phase transitions*, *JHEP* **04** (2021) 055 [2009.10080].
- [43] R.R. Parwani, *Resummation in a hot scalar field theory*, *Phys. Rev. D* **45** (1992) 4695 [hep-ph/9204216].
- [44] D. Curtin, P. Meade and H. Ramani, *Thermal Resummation and Phase Transitions*, *Eur. Phys. J. C* **78** (2018) 787 [1612.00466].
- [45] P.B. Arnold and O. Espinosa, *The Effective potential and first order phase transitions: Beyond leading-order*, *Phys. Rev.*

- D* **47** (1993) 3546 [[hep-ph/9212235](#)].
- [46] G. Hiller and I. Nisandzic, R_K and R_{K^*} beyond the standard model, *Phys. Rev. D* **96** (2017) 035003 [[1704.05444](#)].
- [47] A. Beniwal, M. Lewicki, J.D. Wells, M. White and A.G. Williams, Gravitational wave, collider and dark matter signals from a scalar singlet electroweak baryogenesis, *JHEP* **08** (2017) 108 [[1702.06124](#)].
- [48] E.J. Weinberg and A.-q. Wu, UNDERSTANDING COMPLEX PERTURBATIVE EFFECTIVE POTENTIALS, *Phys. Rev. D* **36** (1987) 2474.
- [49] Measurements of the Higgs boson production and decay rates and constraints on its couplings from a combined ATLAS and CMS analysis of the LHC pp collision data at $\sqrt{s} = 7$ and 8 TeV, .
- [50] CMS collaboration, Measurements of the Higgs boson production and decay rates and constraints on its couplings from a combined ATLAS and CMS analysis of the LHC pp collision data at $\sqrt{s} = 7$ and 8 TeV, .
- [51] ATLAS collaboration, Measurement of the properties of Higgs boson production at $\sqrt{s} = 13$ TeV in the $H \rightarrow \gamma\gamma$ channel using 139 fb^{-1} of pp collision data with the ATLAS experiment, [2207.00348](#).
- [52] CMS collaboration, A portrait of the Higgs boson by the CMS experiment ten years after the discovery, *Nature* **607** (2022) 60 [[2207.00043](#)].
- [53] PARTICLE DATA GROUP collaboration, Review of Particle Physics, *PTEP* **2020** (2020) 083C01.
- [54] CMS collaboration, Sensitivity projections for Higgs boson properties measurements at the HL-LHC, .
- [55] D. d'Enterria, Higgs physics at the Future Circular Collider, *PoS ICHEP2016* (2017) 434 [[1701.02663](#)].
- [56] FCC collaboration, FCC-ee: The Lepton Collider: Future Circular Collider Conceptual Design Report Volume 2, *Eur. Phys. J. ST* **228** (2019) 261.
- [57] P. Bambade et al., The International Linear Collider: A Global Project, [1903.01629](#).
- [58] F. An et al., Precision Higgs physics at the CEPC, *Chin. Phys. C* **43** (2019) 043002 [[1810.09037](#)].
- [59] M. Ruan, Y. Fang, G. Li and D. Yu, CEPC Research Report: Higgs Physics Analysis, [2107.09820](#).
- [60] A. Crivellin, C. Greub, D. Müller and F. Saturnino, Scalar Leptoquarks in Leptonic Processes, *JHEP* **02** (2021) 182 [[2010.06593](#)].
- [61] M. Dine, R.G. Leigh, P.Y. Huet, A.D. Linde and D.A. Linde, Towards the theory of the electroweak phase transition, *Phys. Rev. D* **46** (1992) 550 [[hep-ph/9203203](#)].
- [62] P. Di Bari, D. Marfatia and Y.-L. Zhou, Gravitational waves from first-order phase transitions in Majoron models of neutrino mass, *JHEP* **10** (2021) 193 [[2106.00025](#)].
- [63] CMS collaboration, Search for singly and pair-produced leptoquarks coupling to third-generation fermions in proton-proton collisions at $\sqrt{s} = 13$ TeV, .
- [64] CMS collaboration, Search for singly and pair-produced leptoquarks coupling to third-generation fermions in proton-proton collisions at $s=13$ TeV, *Phys. Lett. B* **819** (2021) 136446 [[2012.04178](#)].
- [65] ATLAS collaboration, Search for pair production of third-generation scalar leptoquarks decaying into a top quark and a τ -lepton in pp collisions at $\sqrt{s} = 13$ TeV with the ATLAS detector, *JHEP* **06** (2021) 179 [[2101.11582](#)].
- [66] ATLAS collaboration, Search for scalar leptoquarks in the $b\tau\tau$ final state in pp collisions at $\sqrt{s} = \sim 13 \text{ TeV}$ with the ATLAS detector, .
- [67] V. Corbin and N.J. Cornish, Detecting the cosmic gravitational wave background with the big bang observer, *Class. Quant. Grav.* **23** (2006) 2435 [[gr-qc/0512039](#)].
- [68] DECIGO WORKING GROUP collaboration, Primordial gravitational wave and DECIGO, *PoS KMI2019* (2019) 019.
- [69] S. Kawamura et al., Current status of space gravitational wave antenna DECIGO and B-DECIGO, *PTEP* **2021** (2021) 05A105 [[2006.13545](#)].
- [70] A. Sesana et al., Unveiling the gravitational universe at μ -Hz frequencies, *Exper. Astron.* **51** (2021) 1333 [[1908.11391](#)].
- [71] M. Hindmarsh, S.J. Huber, K. Rummukainen and D.J. Weir, Numerical simulations of acoustically generated gravitational waves at a first order phase transition, *Phys. Rev. D* **92** (2015) 123009 [[1504.03291](#)].
- [72] A. Megevand and S. Ramirez, Bubble nucleation and growth in very strong cosmological phase transitions, *Nucl. Phys. B* **919** (2017) 74 [[1611.05853](#)].
- [73] E.W. Kolb and M.S. Turner, *The Early Universe*, vol. 69 (1990), [10.1201/9780429492860](#).
- [74] D. Bodeker and G.D. Moore, Can electroweak bubble walls run away?, *JCAP* **05** (2009) 009 [[0903.4099](#)].
- [75] J.R. Espinosa, T. Konstandin, J.M. No and G. Servant, Energy Budget of Cosmological First-order Phase Transitions, *JCAP* **06** (2010) 028 [[1004.4187](#)].
- [76] P.J. Steinhardt, Relativistic Detonation Waves and Bubble Growth in False Vacuum Decay, *Phys. Rev. D* **25** (1982) 2074.
- [77] V.R. Shajiee and A. Tofghi, Electroweak Phase Transition, Gravitational Waves and Dark Matter in Two Scalar Singlet Extension of The Standard Model, *Eur. Phys. J. C* **79** (2019) 360 [[1811.09807](#)].
- [78] R. Zhou, L. Bian and Y. Du, Electroweak phase transition and gravitational waves in the type-II seesaw model, *JHEP* **08** (2022) 205 [[2203.01561](#)].